

October 1998

Single leptoquark production at high-energy e^+e^- colliders

Costas G. Papadopoulos

Institute of Nuclear Physics, NCSR Δημόκριτος, 15310 Athens, Greece

ABSTRACT

A study of the production and the decay of scalar and vector leptoquarks at high-energy e^+e^- colliders is presented. All tree-order contributions to single leptoquark production have been calculated and incorporated in the Monte Carlo event generator ERATO-LQ.

E-mail: Costas.Papadopoulos@cern.ch.

arXiv:hep-ph/9703372v2 19 Jan 1999

PROGRAM SUMMARY

Title of the program: ERATO-LQ.

Catalogue number:

Program obtainable from: Dr. Costas G. Papadopoulos, Institute of Nuclear Physics, NRCPS ‘Democritos’, 15310 Athens, Greece.

Also at <ftp://alice.nrcps.ariadne-t.gr/pub/papadopo/erato>.

Licensing provisions: none

Computer for which the program is designed and others on which it has been tested: HP, IBM, ALPHA and SUN workstations.

Operating system under which the program has been tested: UNIX

Programming language: FORTRAN 77 and FORTRAN 90

Keywords: leptoquark, single leptoquark production, four fermion final states, event generator

Nature of physical problem: Leptoquark states emerge in several theoretical frameworks, including the Pati-Salam model, the MSSM, and composite models of quarks and leptons. Leptoquark states coupled to the first generation leptons and quarks can be studied in e^+e^- colliders. The dominant mode, for leptoquark masses close to the energy threshold, is the single leptoquark production. Leptoquarks can be studied by selecting events with leptons and jets and by investigating the invariant mass distribution of the lepton plus jet system.

Method of solution: Based on the four-fermion event generator ERATO, we have included all possible leptoquark contributions to the processes:

$$e^-e^+ \rightarrow \ell^- \ell^+ q \bar{q}$$

and

$$e^-e^+ \rightarrow \ell^- \bar{\nu}_\ell q \bar{q}' .$$

All tree-order Feynman graphs as well as all necessary phase space mappings have been calculated and incorporated in the present extension ERATO-LQ. Moreover interference terms with the tree-order SM contributions have been fully included. The decay of the leptoquarks has been treated exactly. An additional code providing the total cross section in the resolved photon approximation has also been included.

1 Introduction

Search for new particles has been constantly the center of attention in contemporary high energy physics. The initially reported excess of high Q^2 events at HERA by the H1 [1] and ZEUS [2] collaborations ¹ stimulated a substantial research interest [4, 5, 6, 7] on the possible existence of new particles of leptoquark type. Such particles emerge in several contexts, including the Pati-Salam model [8] and the grand-unified supersymmetric theories [9]. Leptoquark-type interactions, described by higher-dimensional contact terms, are naturally incorporated within the idea of compositeness of quarks and leptons [10].

It is the aim of this paper to present a complete description of the relevant four fermion final states, associated with leptoquark production at high-energy e^+e^- colliders. This automatically includes pair leptoquark production as well as single leptoquark production channels. As a first application we present results concerning single leptoquark production at LEP2.

We start the presentation with the most general effective Lagrangian [16], which is $SU(3) \times SU(2) \times U(1)$ invariant, baryon- and lepton-number conserving as well as family diagonal, in order to avoid the most severe constraints from low-energy considerations [17]. It can be written as

$$\begin{aligned} \mathcal{L}_{F=-2} = & (g_{0L} \bar{q}_L^c i\tau_2 \ell_L + g_{0R} \bar{u}_R^c e_R) S_0 + \tilde{g}_{0R} \bar{d}_R^c e_R \tilde{S}_0 + g_{1L} \bar{q}_L^c i\tau_2 \vec{\tau} \ell_L \vec{S}_1 \\ & + (g_{\frac{1}{2}L} \bar{d}_L^c \gamma^\mu \ell_L + g_{\frac{1}{2}R} \bar{q}_L^c \gamma^\mu e_R) V_{\frac{1}{2}\mu} + \tilde{g}_{\frac{1}{2}L} \bar{u}_R^c \gamma^\mu \ell_L \tilde{V}_{\frac{1}{2}\mu} + \text{cc} \end{aligned} \quad (1)$$

$$\begin{aligned} \mathcal{L}_{F=0} = & (h_{\frac{1}{2}L} \bar{u}_R \ell_L + h_{\frac{1}{2}R} \bar{q}_L i\tau_2 e_R) S_{\frac{1}{2}} + \tilde{h}_{\frac{1}{2}L} \bar{d}_R \ell_L \tilde{S}_{\frac{1}{2}} + \tilde{h}_{0R} \bar{u}_R \gamma^\mu e_R \tilde{V}_{0\mu} \\ & + (h_{0L} \bar{q}_L \gamma^\mu \ell_L + h_{0R} \bar{d}_R \gamma^\mu e_R) V_{0\mu} + h_{1L} \bar{q}_L \vec{\tau} \gamma^\mu \ell_L \vec{V}_{1\mu} + \text{cc} \end{aligned} \quad (2)$$

where $F = 3B + L$ denotes the fermion number. The gauge-interaction terms are given by

$$\mathcal{L} = (D_\mu \Phi)^\dagger D^\mu \Phi - M^2 \Phi^\dagger \Phi \quad (3)$$

for scalars and

$$\mathcal{L} = -\frac{1}{2} G_{\mu\nu}^\dagger G^{\mu\nu} + M^2 \Phi_\mu^\dagger \Phi^\mu \quad (4)$$

for vectors, with

$$G_{\mu\nu} = D_\mu \Phi_\nu - D_\nu \Phi_\mu \quad (5)$$

and the $SU(2)_L \times U(1)_Y$ covariant derivative given by

$$D_\mu = \left[\partial_\mu - ieQ^\gamma A_\mu - ieQ^Z Z_\mu - ieQ^W (W_\mu^+ I^+ + W_\mu^- I^-) \right] \quad (6)$$

where I^\pm are the $SU(2)$ generators in the representation of the corresponding leptoquark state. The electroweak charges are given by

$$Q^Z = \frac{I_3 - Q^\gamma \sin^2 \theta_w}{\cos \theta_w \sin \theta_w} \quad (7)$$

¹For a recent review on leptoquark searches in high Q^2 events at HERA see reference [3]

and

$$Q^W = \frac{1}{\sqrt{2} \sin \theta_w} . \quad (8)$$

In order to account for a more general structure in the vector leptoquark case one can also add the so called ‘anomalous couplings’ terms as for instance the ‘magnetic’ dipole one given by

$$\mathcal{L}_{extra} = -i \sum_{V=\gamma,Z} g_V \kappa_V \Phi_\mu^\dagger V^{\mu\nu} \Phi_\nu \quad (9)$$

parametrized in terms of κ_γ and κ_Z .

2 Single leptoquark production

Leptoquark contributions to e^+e^- processes can be classified into real and virtual ones. To the lowest order, virtual contributions proceed via the reaction $e^+e^- \rightarrow q\bar{q}$ [4, 5, 7], whereas for real ones we have the single leptoquark production mode [18, 19, 20] and for light enough masses, or high enough energies, the pair leptoquark production [21].

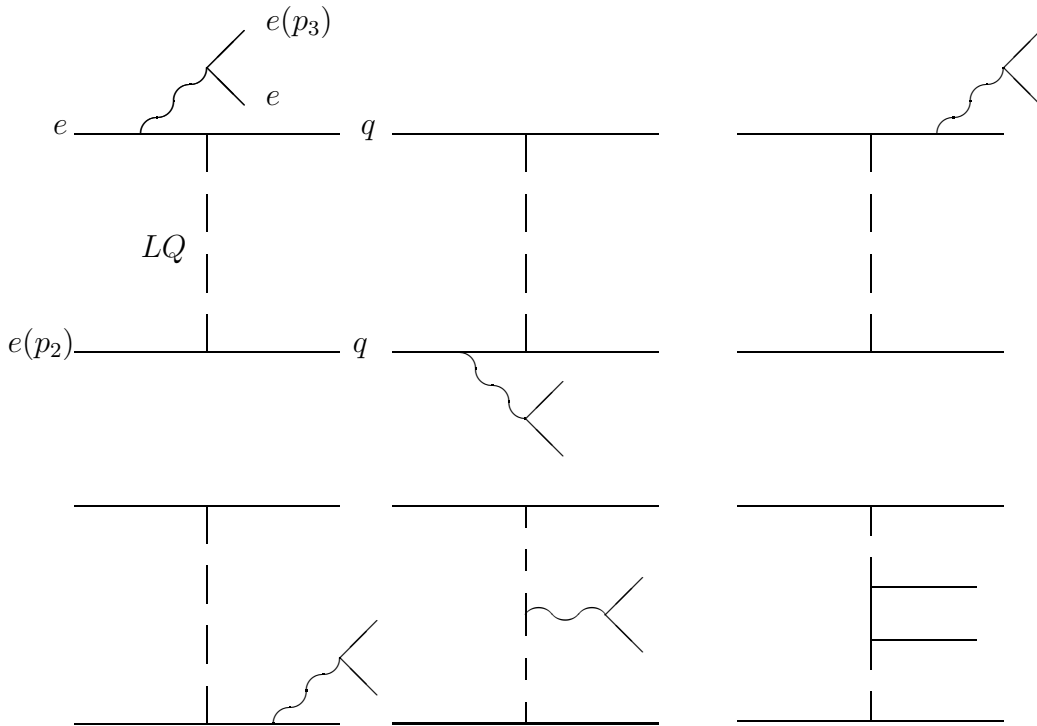


Figure 1: EQ20, EQ10 and EQ5 classes. The curly lines can be γ , Z or W , with the appropriate changes in the fermion species. The other half of the graphs are obtained, as usually, by the interchange $e(p_2) \leftrightarrow e(p_3)$.

Leptoquark production at high-energy e^+e^- collisions results to a four-fermion final state. We have calculated all tree-order contributions, including all interference terms

with the Standard Model, to the following ‘semileptonic’ reactions

$$e^-e^+ \rightarrow \ell^-\ell^+q\bar{q} \quad (10)$$

and

$$e^-e^+ \rightarrow \ell^-\bar{\nu}_\ell q\bar{q}', \quad (11)$$

where $\ell = e, \mu, \tau$. A full description of the MC generator **ERATO** can be found in references [22, 23]. A brief description of its present extension is given in the Appendix. Leptoquark contributions to $\nu_\ell\bar{\nu}_\ell q\bar{q}$ and $q\bar{q}q'\bar{q}'$ final states have not been considered here, since, as we will see, they are relatively suppressed.

For the first reaction, Eq.(10), with $\ell = e$ ($\ell = \mu, \tau$), the Standard Model Feynman graphs are of the NC48 (NC24) type², whereas the leptoquark contribution can be classified in two categories: the LQ22 (LQ11), which is diagrammatically identical to the Standard Model CC22 (CC11) with the W boson replaced by a leptoquark, and a new category, called EQ20, which contributes only when $\ell = e$. The generic graphs belonging to the latter class are shown in Fig.1. Moreover there are nine scalar and nine vector leptoquark states contributing to these processes, namely

$$S_0^L, S_0^R, \tilde{S}_0^R, S_{1+}^L, S_{10}^L, S_{\frac{1}{2}+}^L, S_{\frac{1}{2}+}^R, S_{\frac{1}{2}-}^R \quad \text{and} \quad \tilde{S}_{\frac{1}{2}+}^R$$

and

$$V_{\frac{1}{2}+}^L, V_{\frac{1}{2}+}^R, V_{\frac{1}{2}-}^R, \tilde{V}_{\frac{1}{2}+}^R, V_0^L, V_0^R, \tilde{V}_0^R, V_{1+}^L \quad \text{and} \quad V_{10}^L,$$

with the obvious notation X_{bc}^a , where $a = L, R$ is the helicity of the lepton, $b = I$ is the isospin of the leptoquark and $c = I_3$ stands for its third component.

For the reaction Eq.(11), Standard Model contributions belong to the well known CC20(CC10) category, whereas those of leptoquarks fall into three different classes. The first one is the LQ20(LQ10), in close analogy to the previous case. The other two, the EQ10 and EQ6, Fig.1, receive contributions only from the first generation leptoquarks. In the LQ20(LQ10) class only S_0^L, \vec{S}_1^L and U_0^L, \vec{U}_1^L states contribute, whereas in the classes EQ10 and EQ6 we have contributions from S_1^L, V_1^L and $S_{\frac{1}{2}}^R, V_{\frac{1}{2}}^R$ respectively.

In addition to the calculation of all tree-order Feynman graphs, we have also employed all phase-space mappings [24, 22], which are necessary to cover all the kinematical regions where leptoquarks have the most substantial contributions. Initial state radiation (ISR) has also been included in the structure function approach [25]. Our calculation provides therefore the necessary framework to investigate real leptoquark production at high-energy e^+e^- colliders, including both pair- and single-production modes, for all leptoquark types, as given by Eq.(1)-Eq.(2), and for all generations. Nevertheless we find it convenient, to focus our present analysis on the first generation leptoquarks. It should be mentioned, however, that all necessary contributions for the study of the 2nd and 3rd generation leptoquarks at LEP2 have been fully accounted for in the present calculation.

²For the nomenclature about the four-fermion production diagrams see reference [23].

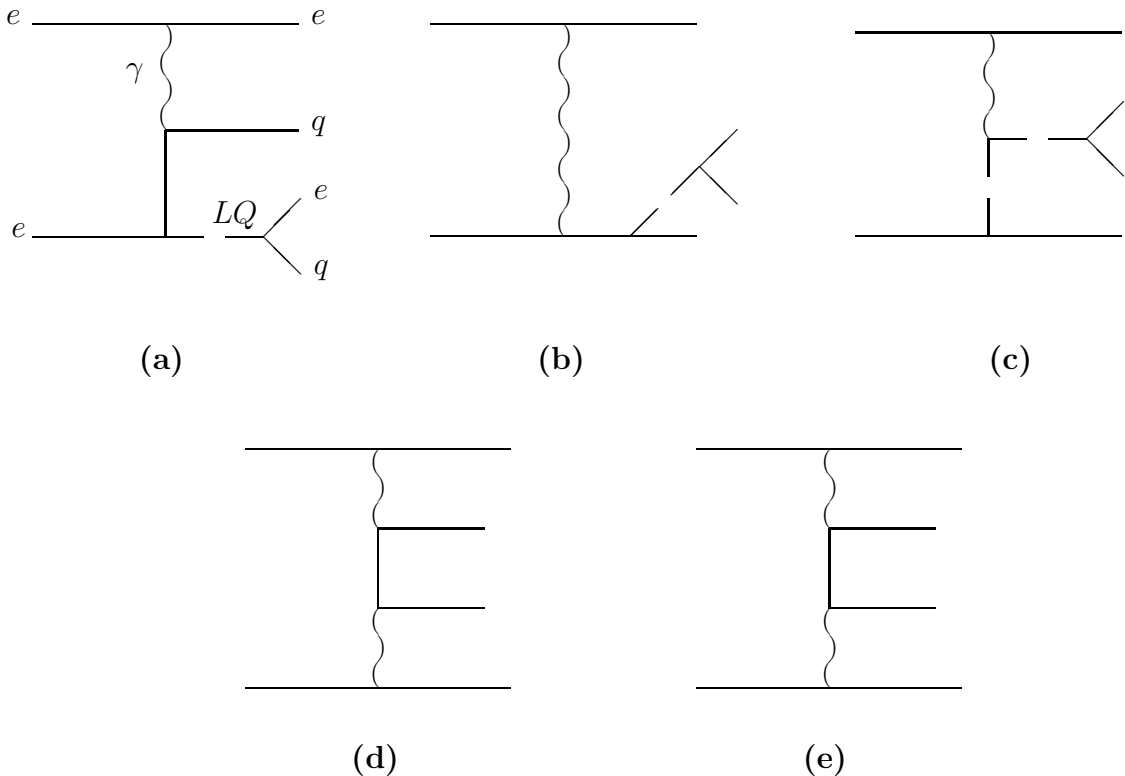


Figure 2: The subset of Feynman graphs giving the dominant contribution to single leptoquark production: (a,b,c) signal, (e,d) background.

Although leptoquark contributions appear in a large number of graphs only a small part of them give a sizable contribution to the production cross-section, depending of course on the leptoquark parameters such as the mass and the Yukawa coupling. The first important consideration is coming from the total width of the leptoquark, which is given by

$$\Gamma_J = f_J \frac{M}{8\pi} \sum_{i=1}^{N_{ch}} \lambda_i^2 \quad (12)$$

where $J = 0, 1$ is the spin of the particle, $f_0 = \frac{1}{2}$ and $f_1 = \frac{1}{3}$ and $N_{ch} = 1$ or 2 depending on how many channels are available. As is evident for a leptoquark mass of the $\mathcal{O}(200 \text{ GeV})$ the typical width is of the order of a few hundreds of MeV. This is mainly due to the fact that leptoquarks couple to ordinary fermions in a very restricted way, which is not generally true for other types of leptoquark couplings, like those appearing in R-parity violating MSSM [4]. As a consequence of the narrowness of these states the interference terms among resonant and non-resonant contributions are rather suppressed.

The second remark is that, for leptoquark masses $M \geq \sqrt{s}/2$, the single leptoquark production mode becomes dominant as far as the first generation leptoquarks are con-

cerned. This proceeds mainly via the t -channel graphs, shown in Fig.2, and their contribution comes mainly from the collinear electrons (positrons). This can be described either by the Weizsäcker-Williams [26] approximation or by integrating over the momentum of the final state electron using the leading logarithmic approximation as described in reference [24]. We have implemented *both* approaches, and checked that the results agree within less than 10%, which is rather typical for the leading logarithmic (LL) approximation we are essentially employing in both cases. As far as the Weizsäcker-Williams spectrum is concerned, we have used the following form:

$$f_{\gamma/e}(x, s) = \frac{\alpha}{2\pi} \left[\frac{1 + (1-x)^2}{x} \ln \left(\frac{s}{m_e^2} \frac{(1-x)^2}{(2-x)^2} \right) + x \ln \frac{2-x}{x} + \frac{2(x-1)}{x} \right]. \quad (13)$$

It should be mentioned that this type of contributions, which are substantially enhanced due to the t -channel photon exchange, are only relevant for the first generation leptoquarks and for the semileptonic reactions, Eq.(10)-Eq.(11), under consideration. On the other hand, first generation leptoquark contributions to $\nu_\ell \bar{\nu}_\ell q \bar{q}$ and $q \bar{q} q' \bar{q}'$ final states are relatively suppressed, due to the absence of the t -channel photon exchange enhancement.

Finally, as the first graph of Fig.2 has a mass singularity in the quark propagator, special care has to be paid in the integration in this specific case. As before the LL-approximation scheme has been employed. It is worth to mention that comparing with the exact result for the total cross-section [19], taking into account the quark masses³, and properly integrating over the photon spectrum, both results agree to less than a few percent. Moreover in order to have a quantitative estimate of the QCD effects, due to the presence of the light quark mass singularity, we compare the perturbative results with the resolved photon contribution. In the latter case the total cross section for the single-leptoquark production is given by

$$\sigma(e^+ + e^- \rightarrow S_0 + X) = \int dx dz f_{\gamma/e}(x, s) f_{q/\gamma}(z, M_{LQ}^2) \hat{\sigma}(xzs) \quad (14)$$

which can be written as

$$\sigma(e^+ + e^- \rightarrow S_0 + X) = \frac{\pi^2 \alpha_{em}}{s} \left(\frac{\lambda}{e} \right)^2 \int_{M_{LQ}^2/s}^1 \frac{dx}{x} f_{\gamma/e}(x, s) f_{q/\gamma}(M_{LQ}^2/(xs), M_{LQ}^2) \quad (15)$$

where $f_{q/\gamma}$ is the structure function of the quark inside the photon. In Fig.3 we show the cross section as a function of the leptoquark mass for $\sqrt{s} = 192$ GeV, for two different choices of the structure function parametrizations [27] compared to the perturbative calculation. We see that, even in the total cross section, one can safely trust the perturbative estimate. Moreover this exercise shows us that an error of the order of 10% to 20% is to be expected, whereas the differences between the two schemes are concentrated in the mass region near the kinematical threshold.

³For the light quarks we take $m_{(u,d)} = 300$ MeV.

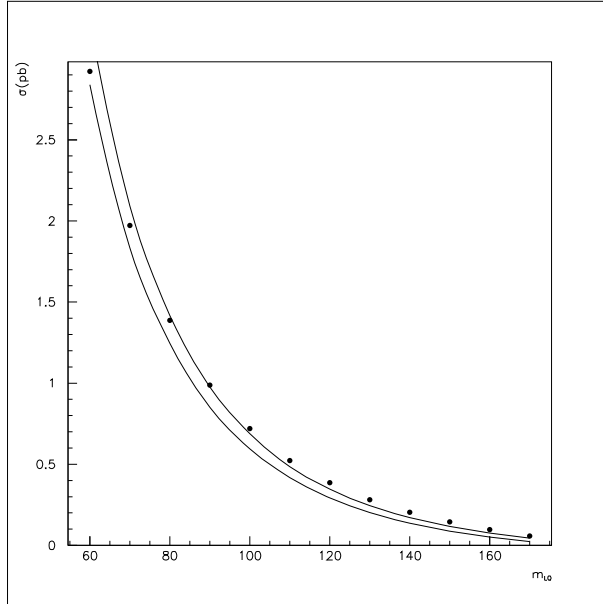


Figure 3: Total cross section for single-leptoquark production, S_0 (u-type) as a function of the leptoquark mass, for $\lambda/e = \frac{1}{2}$. The solid lines represent the resolved photon contribution (upper: SAS-G 1D, lower: DO-G Set1) whereas points refer to the perturbative result with light quark mass 300 MeV.

3 Results & Discussion

After completing the description of our calculation, we now come to the physics picture emerging from it. In the case of NC-type final states, Eq.(10), the signal has the typical structure of a lepton and a jet balancing each other's transverse momentum with some hadronic activity in the forward (backward) region. In the irreducible Standard Model background, on the other hand, the angular distribution of the positron (electron) is peaking in the backward (forward) direction. In order to suppress as much as possible the background, without lowering signal's contribution, we have employed the following set of cuts:

$$m_{e-jet} \geq 140 \text{ GeV} , \quad 5^\circ \leq \max(\theta_{j1}, \theta_{j2}) \leq 175^\circ , \quad 20^\circ \leq \theta_e \leq 160^\circ , \quad E_e \geq 5 \text{ GeV} . \quad (16)$$

Among them the most important ones are the cut on the angle of the observed positron (electron) and the cut on the electron-jet invariant mass, m_{e-jet} . In Fig.4 we show the invariant mass, m_{e-jet} , distribution for leptoquark mass $M = 170 \text{ GeV}$ and $\lambda/e = 0.5$, with an integrated luminosity $L = 500 \text{ pb}^{-1}$.

In the case of CC-type final states, Eq.(11), the signal, which is much more spectacular, consists only of one very energetic jet and a large amount of missing transverse energy.

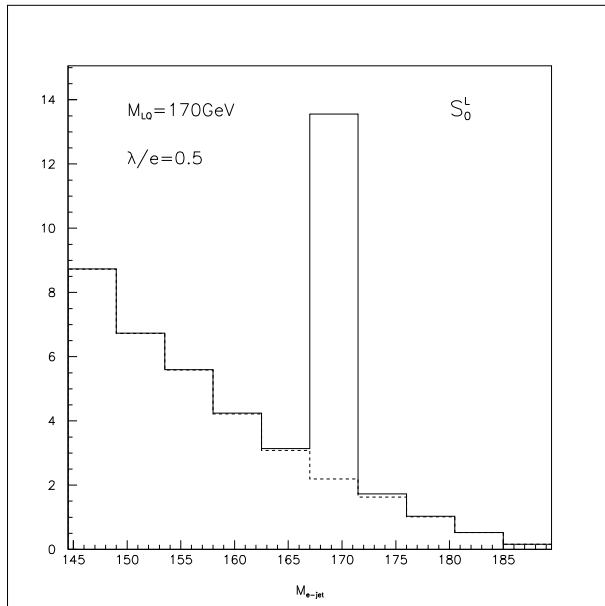


Figure 4: The m_{e-jet} invariant mass distribution in number of events per bin.

The only cuts employed in this case are

$$\max(p_{T1}, p_{T2}) \geq 60 \text{ GeV} \quad , \quad \min(\theta_{j1}, \theta_{j2}) \leq 5^\circ \text{ or } \geq 175^\circ \quad , \quad (17)$$

where p_T is the transverse energy of the jet. The second cut is employed in order to reduce the main irreducible background contribution, coming from single W production, in which case two energetic jets, with an invariant mass $\mathcal{O}(M_W)$, would be present in the final state at relatively large angles with respect to the beam. Moreover, as the only kinematical information available in this channel is the jet momentum, one cannot fully reconstruct the mass of the leptoquark state, due to the missing neutrino energy⁴. In Fig.5 we show the p_T spectrum of the signal as well as that of the irreducible Standard Model background.

In summary, we have presented a calculation of leptoquark contributions to two- and four-fermion final states at e^+e^- collisions, which has been incorporated in the MC event generator ERATO. Taking into account the Standard Model irreducible backgrounds we have presented a first study of single leptoquark production, in both its NC or CC channel at LEP2 energies.

⁴However the leptoquark mass can still be determined by the endpoint of the p_T spectrum.

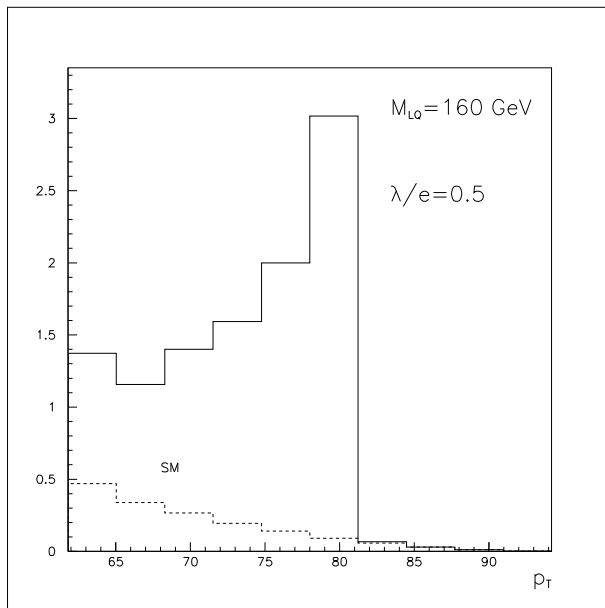


Figure 5: The p_T distribution in number of events per bin.

Appendix: The program ERATO-LQ

In this appendix we briefly describe the program ERATO-LQ. The skeleton of the program follows closely the skeleton of the mother program ERATO [22]. The distributed code contains two main directories, `ffiles` where all FORTRAN files are stored and `run` where the input files as well as the `makefile` resides. There are two main FORTRAN files, `lqq.f` and `vud.f` corresponding to $e^+e^- \rightarrow e^-e^+q\bar{q}$ and $e^+e^- \rightarrow e^-\bar{\nu}_e u\bar{d}$ processes respectively. The files `algor.f`, `alice.f` and `common.f` contains all necessary routines to make the program run⁵. The input files look like:

```

7,1,1,0      !process,scalar or vector
3           !iterations
1           !ISR
128.07 0.2310309 91.1888 2.4974 80.23 2.033 !input parameters
1           !itotal
-1. 0.1     !cmax(cmin) cmas
192        !energy

```

⁵Random number generator and the gamma function $\Gamma(x)$ are obtained from the Cern Library, CERLIB.

```

50000          !nev
145. 0.5       !LQ parameters : mass and 1/e
10000.         !scut = (mass-10)**2
2000          !IEV
1             !iopt :=0 no optimization
4000 6000 10000 15000 20000 30000 120000 250000 500001
100.          !cut on invariant mass l+q= mass-10
0.3           !mass of light quark
20. 5. 5. 5. 5. 25.    !angles=degrees: clmax cjmax eelmin ejmin c4max cmas
1             !naive

```

which is very much the same as the one used by ERATO [22]. The new variables used in the present code, in addition to those already described in reference [22], are:

- **IPRO**
This is used to select the corresponding process: IPRO=5 selects $e^+e^- \rightarrow e^-e^+u\bar{u}$, IPRO=6 $e^+e^- \rightarrow e^-e^+d\bar{d}$.
- **ICHOICE**
This is used to select the specific leptoquark (charge, decay mode) as described in Table 1 and Table 2.
- **ISCALAR**
ISCALAR=1 if a scalar leptoquark is selected.
- **IVECTOR**
IVECTOR=1 if a vector leptoquark is selected.
- **RLQMAS**
The mass of the leptoquark.
- **CLQ**
The leptoquark coupling, $g_L(g_R)$, as described in Table 1 and Table 2, normalized to the electromagnetic one, i.e, $g_L \leftarrow 1$ means $g_L = e$, $e = \sqrt{4\pi\alpha_{em}}$.
- **QMAS**
This is the value of the light quark mass used as regulator of the IR divergences of the amplitude. By default is set equal to 300 MeV.

The final-state kinematics is represented by the three momenta, $p_4(e^+)$, $p_3(u)$ and $p_{10}(d)$. Variable `clmax` is the minimum angle allowed between the momentum p_4 and the beam; `cjmax` the minimum angle (in degrees) allowed between the hardest jet (p_3 or p_{10}) and the beam; `eelmin` is the minimum energy of p_4 ; `ejmin` is the minimum energy of the hardest jet; `c4max` is the minimum angular separation between the hardest jet and

the lepton; `cmass` is the minimum invariant mass of the two-jet system. If `NITER=3` then the output provides cross sections for the signal process (`ITER=1`) and for the Standard Model contribution (`ITER=2`). In addition, the total cross section for on-shell leptoquark production is given (`ITER=3`), where the decay process of the leptoquark has not been taken into account and no phase-space cut has been applied.

Finally a typical output of the `lqq.f` code, corresponding to the input described above, looks as follows:

```

                TOTAL SIGMA IN NB          ERROR
LQ ERATO      1.749165382052100E-05  3.148577170490561E-07
LQ:  on-shell 3.939744840638816E-05  3.045651348671309E-07
SM          1.206926939341498E-04  7.367659234150230E-05
[TOTAL,PASS,FAIL,ICUT]   :   50000  9951 40049 29398  1152  2645  6854

```

In addition a programme called `phot.f` which calculates the total cross section from the resolved photon contribution, Eq.(15), is provided. All the leptoquark coupling (see Table 1 and Table 2) have been incorporated. A link to the standard parton distribution functions library, `PDFLIB`, is assumed.

LQ	ICHOICE	Q	Decay Mode	BR	Coupling
S_0^L	1	$-\frac{1}{3}$	$e_L u$ $\nu_L d$	$\frac{1}{2}$	g_L $-g_L$
S_0^R	2	$-\frac{1}{3}$	$e_R u$	1	g_R
\tilde{S}_0^R	3	$-\frac{4}{3}$	$e_R d$	1	g_R
S_{1+}^L	4	$-\frac{4}{3}$	$e_L d$	1	$-\sqrt{2} g_L$
S_{10}^L	5	$-\frac{1}{3}$	$e_L u$ $\nu_L d$	$\frac{1}{2}$	$-g_L$ $-g_L$
$S_{\frac{1}{2}+}^L$	6	$-\frac{5}{3}$	$e_L \bar{u}$	1	g_L
$S_{\frac{1}{2}+}^R$	7	$-\frac{5}{3}$	$e_R \bar{u}$	1	g_R
$S_{\frac{1}{2}-}^R$	8	$-\frac{2}{3}$	$e_R \bar{d}$	1	$-g_R$
$\tilde{S}_{\frac{1}{2}+}^R$	9	$-\frac{2}{3}$	$e_L \bar{d}$	1	g_L

Table 1: Scalar leptoquark charges, couplings and decay modes, as used by ERATO-LQ

LQ	ICHOICE	Q	Decay Mode	BR	Coupling
$V_{\frac{1}{2}+}^L$	1	$-\frac{4}{3}$	$e_L d$	1	g_L
$V_{\frac{1}{2}+}^R$	2	$-\frac{4}{3}$	$e_R d$	1	g_R
$V_{\frac{1}{2}-}^R$	3	$-\frac{1}{3}$	$e_R u$	1	g_R
$\tilde{V}_{\frac{1}{2}+}^R$	4	$-\frac{1}{3}$	$e_L u$	1	g_L
V_0^L	5	$-\frac{2}{3}$	$e_L \bar{d}$ $\nu_L \bar{u}$	$\frac{1}{2}$	g_L g_L
V_0^R	6	$-\frac{2}{3}$	$e_R \bar{d}$	1	g_R
\tilde{V}_0^R	7	$-\frac{5}{3}$	$e_R \bar{u}$	1	g_R
V_{1+}^L	8	$-\frac{5}{3}$	$e_L \bar{u}$	1	$\sqrt{2} g_L$
V_{10}^L	9	$-\frac{2}{3}$	$e_L \bar{d}$ $\nu_L \bar{u}$	$\frac{1}{2}$	$-g_L$ g_L

Table 2: Vector leptoquark charges, couplings and decay modes, as used by ERATO-LQ

References

- [1] H1 Collaboration, C.Adloff *et al.*, Z.Phys. **C74** (1997) 191-206, hep-ex/9702012.
- [2] ZEUS Collaboration, J.Breitweg *et al.*, Z.Phys. **C74** (1997) 207-220, hep-ex/9702015.
- [3] ‘A Search for Leptoquark Bosons in DIS at High Q^2 at HERA’, H1 Collaboration, ICHEP98-579, presented in ICHEP98, Vancouver, Canada.
‘Search for narrow high mass states in positron-proton scattering at HERA’, Zeus Collaboration, ICHEP98-754, presented in ICHEP98, Vancouver, Canada.

- [4] D. Choudhury, S. Raychaudhuri, Phys.Lett. **B401** (1997) 54-61 ; G. Altarelli *et al.*, Nucl.Phys. **B506** (1997) 3-28 ; H. Dreiner and P. Morawitz, Nucl.Phys. **B503** (1997) 55-78.
- [5] J. Kalinowski, R. Rückl, H. Spiesberger and P.M. Zerwas, Z.Phys. **C74** (1997) 595-603, hep-ph/9703288.
- [6] J. Blümlein, Z.Phys. **C74** (1997) 605-609, hep-ph/9703287; K.S. Babu, C. Kolda, J. March-Russel, and F. Wilczek, Phys.Lett. **B402** (1997) 367-373, hep-ph/9703299; V. Barger, K. Cheung, K. Hagiwara and D. Zeppenfeld, Phys.Lett. **B404** (1997) 147-152, hep-ph/9703311.
- [7] J.L. Hewett and T.G. Rizzo, Phys.Rev. **D56** (1997) 5709-5724, hep-ph/9703337.
- [8] J.C. Pati and A. Salam, Phys. Rev. **D8** (1973) 1240; *ibid* **D10** (1974) 275.
- [9] H. Georgi and S.L. Glashow, Phys. Rev. Lett. **32** (1974) 438; P.Langacker, Phys. Rep. **72** (1981) 185 ; E.Witten, Nucl. Phys. **B258** (1985) 75; J.L. Hewett and T.G. Rizzo, Phys. Rep. **193** (1989) 193
- [10] L. Abbot and E. Farhi, Phys. Lett. **B101** (1981) 69; W. Buchmüller, Acta Phys. Austr. Suppl. XXVII (1985)517; H. Harari and N. Seiberg, Phys. Lett. **B98** (1981) 269; S. Adler, IASSNS-HEP-97/12, hep-ph/9702378.
- [11] B. Abbot *et al.*, D0 Collaboration, Phys.Rev.Lett. **79** (1997) 4321-4326, hep-ex/9707033.
- [12] F. Abe *et al.*, CDF Collaboration, Phys. Rev. Lett. **79**, (1997) 4327.
- [13] F. Abe *et al.*, CDF Collaboration, Phys. Rev. Lett. **78** (1997) 2906 and Phys. Rev. Lett. **75** (1995) 1012.
- [14] H1 Collaboration, S. Aid *et al.*, Phys. Lett. **B369** (1996) 173; ZEUS Collaboration, M. Derrick *et al.*, Phys. Lett. **B306** (1993) 173 and Z. f. Phys. **C73** (1997) 613.
- [15] OPAL Collaboration, OPAL Physics Note 288, contributing paper LP138 to the XVIII International Symposium on Lepton-Photon Interactions, Hamburg, 1997.
- [16] W. Buchmüller, R. Rückl and D. Wyler, Phys. Lett. **B191** (1987) 442.
- [17] M. Leurer, Phys. Rev. **D49** (1994) 333; *ibid* **D50** (1994) 536.
- [18] M.A. Doncheski and S. Godfrey, Phys.Lett. **B393** (1997) 355-359, hep-ph/9608368, *ibid* Mod.Phys.Lett. **A12** (1997) 1719-1725, hep-ph/9703285.
- [19] G. Bélanger, D. London and H. Nadeau, Phys. Rev. **D49** (1994) 3140.

- [20] T.M. Aliev, E. Iltan and N.K. Pak, *Phys. Rev.* **D54** (1996) 4263.
- [21] J. Blümlein and R. Rückl, *Phys. Lett.* **B304** (1993) 337 and references therein;
J. Blümlein, E. Boos and A .Kryukov, *Phys. Lett.* **B392** (1997) 150.
- [22] Costas G. Papadopoulos, *Comp.Phys.Comm.* **101** (1997) 183.
`ftp://alice.nrcps.ariadne-t.gr/pub/papadopo/erato.`
- [23] D. Bardin *et al.*, ‘Event generators for *WW* physics’ in *Physics at LEP2*, ed.
G. Altarelli *et al.*, Vol.2, p. 3, CERN 96-01, February 1996, `hep-ph/9709270`.
- [24] F.A.Berends, R.Pittau and R.Kleiss, *Nucl.Phys.***B424**(1994) 308.
- [25] W. Beenakker *et al.*, ‘*WW* cross sections and distributions’ in *Physics at LEP2*, ed.
G. Altarelli *et al.*, Vol.1, p. 79, CERN 96-01, February 1996 & `hep-ph/9602351`.
- [26] C.F. von Weizsäcker, *Z. Phys.* **88**(1934), 612; E.J. Williams, *Phys. Rev.* **45** (1934)
729; M. Chen and P. Zerwas, *Phys. Rev.* **D12** (1975) 187.
- [27] H. Blothow-Besch, *Int. J. Mod. Phys.* **A10** (2901) 1995.